
**FABRICATION, TREATMENT, AND TESTING
OF MATERIALS AND STRUCTURES**

Influence of the Synthesis Conditions and Tin Nanoparticles on the Structure and Properties of a -C:H⟨Sn⟩ Composite Thin Films

A. P. Ryaguzov^{a,*}, R. R. Nemkayeva^a, and N. R. Guseinov^a

^aNational Nanotechnology Laboratory of Open Type (NNLOT), Kazakh National University, Almaty, 050040 Kazakhstan

*e-mail: ryaguzov_a@mail.ru

Submitted December 5, 2017; accepted for publication January 29, 2018

Abstract—The results of studies of the structure and properties of composite materials based on amorphous carbon (a -C:H) films and tin nanoparticles are reported. The composite films are synthesized by the magnetron-assisted ion-plasma sputtering of a combined target in a 92%Ar : 4%CH₄ : 4%H₂ gas mixture. The dependence of the local structure of the a -C:H⟨Sn⟩ films on the conditions of synthesis and the content of Sn nanoparticles is clarified by means of Raman spectroscopy. The dependence of the photoluminescence intensity and the optical band gap of a -C:H⟨Sn⟩ films on the Sn content is shown.

DOI: 10.1134/S1063782618100172

1. INTRODUCTION

The large variety of properties of crystalline carbon is defined by certain spatial arrangements of C–C bonds and by types of their hybridization. At the same time, of particular interest are the structure and properties of amorphous carbon. Over the last three decades, special attention has been given to the study of amorphous diamond-like carbon (DLC) films. Due to their high strength and chemical inertness to corrosive media, DLC films have found wide application as antifriction and durable coatings [1, 2] with good adhesive characteristics.

At present, the problem of controlling electronic processes in hydrogenated amorphous carbon (a -C:H) films still remains urgent. The electronic processes depend on the distribution of the band electron density of states (DOS) defined by the atomic structure of a -C:H films. It is known that the formation of the atomic structure of a material depends on many factors. When creating certain structures for nanoelectronics, one must take into consideration the interactions of the substrate surface with adatoms of the growing film; these interactions are defined mainly by electrostatic forces [3]. The state and structure of the substrate surface have a profound effect on the formation of the film [4]. In addition, a special role in the formation of the atomic structures of films is played by the thermodynamic conditions of synthesis [5]. With the use of the magnetron-assisted ion-plasma method of synthesis, it is possible to implement the structural and impurity modification of a -C:H films over a wide range of thermodynamic parameters and, thus, to control the electronic properties of the films.

Carbon is one of a few elements that do not form chemical bonds with a rather large number of substances in a wide range of synthesis conditions. This property makes it possible to form nanoparticles in a carbon matrix. Carbon films modified with nanoparticles of a substance incapable of forming carbides constitute a certain class of composites with unique properties. Due to quantum-confinement effects, nanoparticles can possess new properties that greatly differ from the properties of these materials >100 nm in dimensions. For example, silver, gold, or platinum nanoparticles in a carbon matrix exhibit plasmon absorption resonance and the percolation mechanism of conduction [6–9], which is predominantly defined by quantum states of the electron substructure of nanoparticles. Composite materials are extensively studied and find increasing applications [10–14]. The possibility of controlling electronic processes in composite materials based on amorphous carbon films will allow extension of the field of their use, specifically for the production of high-sensitivity sensors, new nanoelectronic and optoelectronic devices, etc.

In this study, to modify carbon films, we choose tin which belongs to elements incapable of forming carbides and can exist in two modifications: (i) grey tin (α -Sn) which is diamond-like in atomic structure and belongs to semiconductors and (ii) white tin (β -Sn) which is a plastic metal, whose atomic structure is tetragonal. Depending on the conditions of synthesis and the content and size of Sn nanoparticles, they can form the α or β structural modification. Therefore, tin nanoparticles can influence the formation of the structure of the carbon matrix and its electronic properties in different ways.

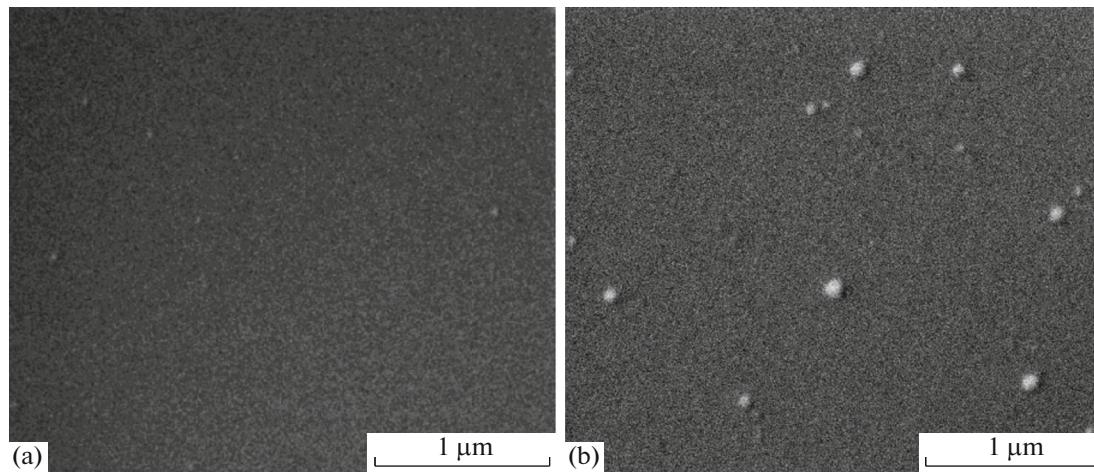


Fig. 1. SEM micrographs of the surface of $a\text{-C:H(Sn}_x\text{)}$ films with $X_{\text{Sn}} =$ (a) 0 and (b) 3.18 at %.

In this paper, we report the results of studies of the structure and properties of synthesized films in relation to the conditions of synthesis and the Sn content. Based on concepts of the sp^2 and sp^3 hybridization of C–C bonds in the carbon matrix and on the notion on the α and β modifications of Sn nanoparticles, we propose an interpretation of the luminescence and optical properties of $a\text{-C:H(Sn)}$ films.

2. EXPERIMENTAL

The $a\text{-C:H(Sn}_x\text{)}$ composite films were produced by the DC magnetron-assisted ion-plasma sputtering of a combined target in a 92%Ar : 4%CH₄ : 4%H₂ gas mixture. The magnetic field of the magnetron was created with a DC electromagnet. Correction of the magnetic-field strength allowed us to maintain the plasma-discharge voltage and current constant during film synthesis. The purity of gases and the graphite target corresponded to 99.999%, and the purity of tin was 99.98%. The $a\text{-C:H(Sn}_x\text{)}$ films were synthesized at a pressure of 0.7 Pa and the substrate temperatures $T_{\text{sub}} = 50$ and 250°C. The specific power of the DC ion-plasma discharge was $P_d = 2.5 \text{ W cm}^{-2}$. The films were synthesized simultaneously on silicon (Si(100)) and quartz (SiO₂) wafers. The average growth rate of the films was $\sim 0.2 \text{ \AA s}^{-1}$. The film thickness was $60 \pm 10 \text{ nm}$, depending on the conditions of synthesis. It should be noted that, at the substrate temperature $T_{\text{sub}} = 250^\circ\text{C}$, the process of growth of the film involves, apart from sputtering of the target with argon ions, an intense process of thermally activated chemisorption induced by the decomposition of methane molecules.

The thickness and surface structure of the films synthesized were studied with a Quanta 200i 3D (FEI company) scanning electron microscope (SEM).

Raman spectroscopy was used to study the structure of the films in relation to the conditions of their synthesis. In Raman measurements, we used an NTegra Spectra (NT-MDT, Russia) setup and a laser emitting at the wavelength $\lambda = 473 \text{ nm}$. The Sn content X_{Sn} was determined by energy-dispersive X-ray microanalysis (energy-dispersive spectroscopy (EDS)) with an accuracy of ± 0.01 at %. The optical transmittance and reflectance spectra were studied with a UV-3600 (Shimadzu, Japan) spectrophotometer.

3. RESULTS AND DISCUSSION

SEM studies of the surface structure of $a\text{-C:H(Sn}_x\text{)}$ films show that tin forms spherically shaped nanoparticles 10–80 nm in dimensions and the number of these nanoparticles per unit area is different, depending on the Sn content. Figure 1 shows micrographs of a pure film and a film containing the tin impurity. The films were synthesized on silicon substrates at $P_d = 2.5 \text{ W cm}^{-2}$ and $T_{\text{sub}} = 50^\circ\text{C}$. Figure 2 shows the EDS spectra for a pure $a\text{-C:H}$ film and a Sn-containing $a\text{-C:H(Sn}_x\text{)}$ film synthesized on silicon.

Raman spectroscopy reveals a difference between the local structures of the $a\text{-C:H}$ and $a\text{-C:H(Sn}_x\text{)}$ films synthesized on Si(100) and SiO₂ wafers. It is known [15, 16] that the Raman spectra of carbon structures exhibit two principal peaks, the G peak in the frequency range 1500–1600 cm^{-1} and the D peak in the range 1350–1450 cm^{-1} . Figure 3 shows the Raman spectra of the $a\text{-C:H}$ and $a\text{-C:H(Sn}_x\text{)}$ films. From Fig. 3, it can be seen that the Sn content influences the formation of the local structure of the carbon matrix. The effect of the thermodynamic and kinetic conditions of synthesis on the properties of the $a\text{-C}$ and $a\text{-C:H}$ films was considered in more detail elsewhere [4, 17].

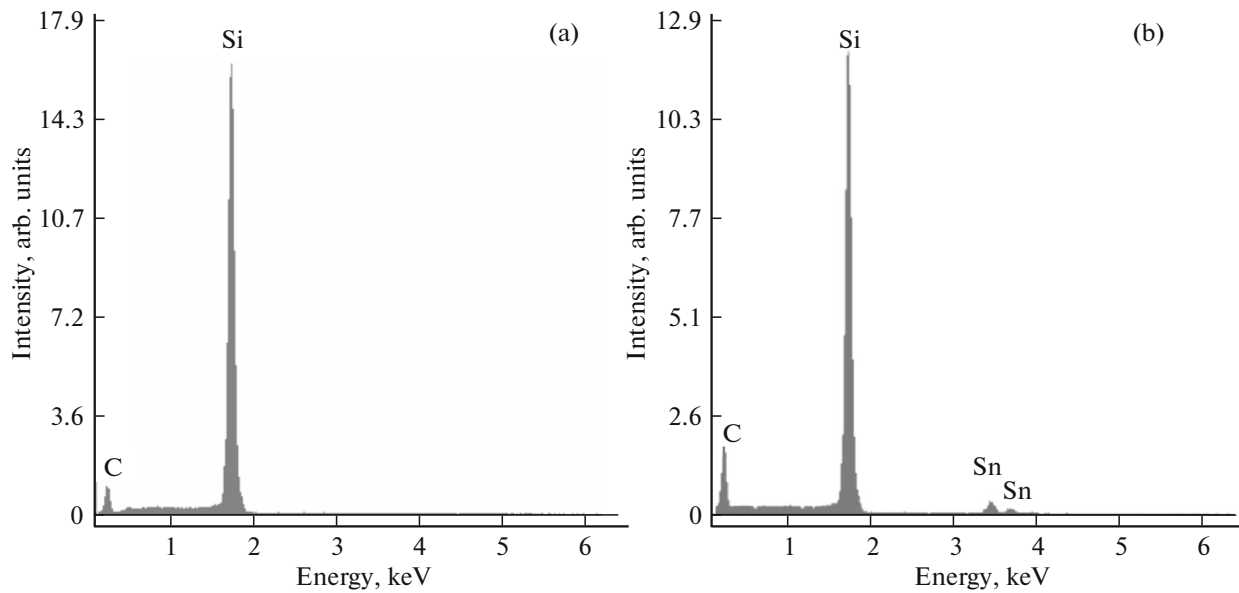


Fig. 2. EDS spectra of $a\text{-C:H(Sn}_x\text{)}$ films with $X_{\text{Sn}} =$ (a) 0 and (b) 3.18 at %.

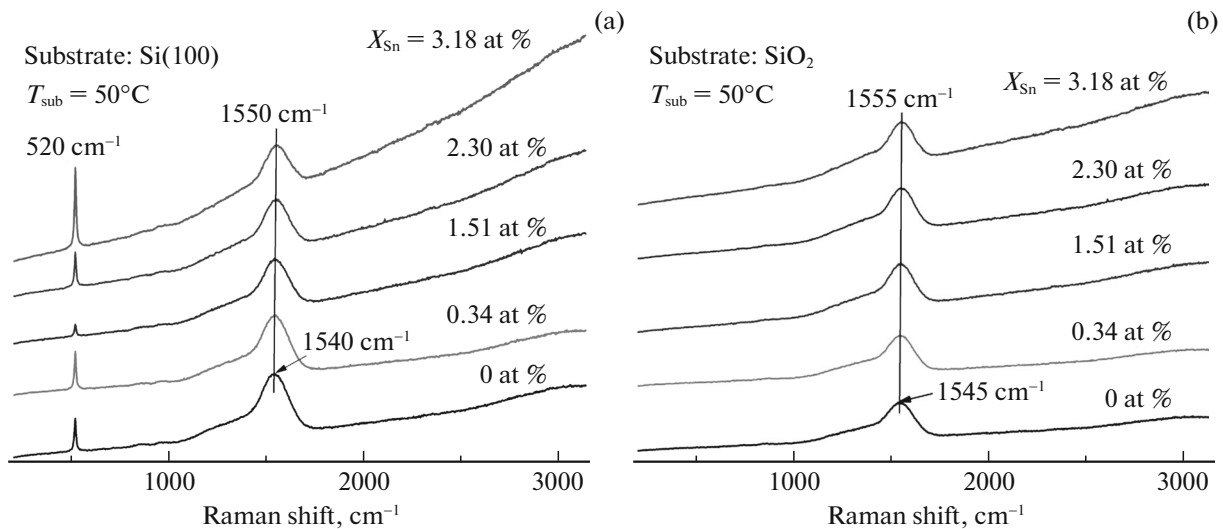


Fig. 3. Raman spectra of $a\text{-C:H(Sn}_x\text{)}$ films synthesized on (a) silicon and (b) quartz substrates.

An increase in the Sn content yields a shift of the G peak to higher frequencies and an increase in the slope of the Raman spectrum. The last-mentioned effect is defined by an increase in the photoluminescence (PL) intensity. The shift of the G peak to higher frequencies is indicative of an increase in the number of sp^2 sites in the amorphous $a\text{-C:H(Sn}_x\text{)}$ film; i.e., the structure of the film is graphitized. When comparing Figs. 3a and 3b, we can see that, at equal Sn fractions, the G peak in the films on SiO_2 substrates is shifted to the high-frequency region by 5 cm^{-1} . Such a shift is indicative of a difference between the fractions of

sp^2 sites, but the slope of the Raman curve for the $a\text{-C:H(Sn}_x\text{)}$ films synthesized on SiO_2 substrates is smaller than that for the films on Si(100) substrates. The difference between the slopes of the PL background can be attributed to a difference between the emission intensities. The number of radiative transitions depends on the distribution of the density of localized states in the bands, which in turn is defined by the atomic structure of the film. The formation of the atomic structure of $a\text{-C:H(Sn}_x\text{)}$ films under these conditions of synthesis depends on the distribution of the surface potential of the substrate and, in addition, on the Sn content, as is evident from Fig. 3. The

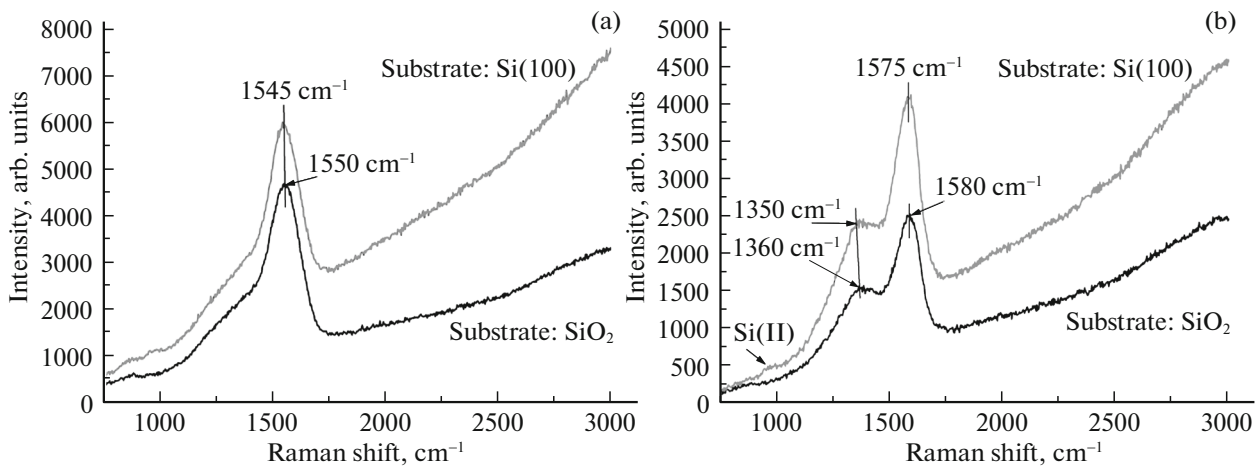


Fig. 4. Raman spectra of $a\text{-C:H}\langle\text{Sn}_x\rangle$ films synthesized at substrate temperatures of (a) 50 and (b) 250°C. $X_{\text{Sn}} = 1.5 \pm 0.2$ at %; $P_d = 2.5 \text{ W cm}^{-2}$.

Si(100) crystal surface is favorable for the formation of sp^3 sites, as suggested by the shift of the G peak to lower frequencies.

Another important parameter that influences the formation of the structure of $a\text{-C:H}\langle\text{Sn}_x\rangle$ films is the substrate temperature. The dependences of the Raman spectra of $a\text{-C:H}\langle\text{Sn}_x\rangle$ films on different substrates on the substrate temperature is illustrated in Fig. 4. It can be seen that an increase in T_{sub} results in a substantial (30 cm^{-1}) shift of the G peak to higher frequencies, which suggests an increase in the number of sp^2 sites. The position of the G peak in films synthesized at 250°C corresponds to 1575 cm^{-1} in the case of Si substrates and to 1580 cm^{-1} in the case of SiO_2 substrates. These Raman frequencies are characteristic of highly oriented pyrolytic graphite and polycrystalline graphite [15, 18]. In the crystals, the full width at half-maximum of the G peak (FWHM_G) is $10\text{--}30 \text{ cm}^{-1}$, which is indicative of ordering of the atomic structure [19]. In Fig. 4, the FWHM_G is ~ 180 and $\sim 150 \text{ cm}^{-1}$ at $T_{\text{sub}} = 50$ and 250°C , respectively. The values of the FWHM_G in $a\text{-C:H}\langle\text{Sn}_x\rangle$ films are much larger than the corresponding values in crystals [19], suggesting a high degree of disorder of the atomic structure. The appearance of the D peak is associated with the breathing mode of the C_6 hexagonal molecule, and this is possible, only if two or three degrees of freedom appear. Therefore, the breathing mode of the C_6 molecule can appear in a disordered atomic structure. In the $a\text{-C:H}\langle\text{Sn}_x\rangle$ films synthesized at 250°C, the D peak is more pronounced, which corresponds to a higher percent content of graphite crystal clusters in the amorphous carbon matrix compared to the content in the films synthesized at 50°C.

We studied the local structure of the $a\text{-C:H}\langle\text{Sn}_x\rangle$ films synthesized at a temperature of 250°C. At this temperature of synthesis, tin nanoparticles have no effect on the shape of the Raman spectrum and the position of the G peak; i.e., at the temperature 250°C, the influence of tin nanoparticles on the formation of the atomic structure of the amorphous carbon matrix is suppressed. In addition, we can note the influence of the material and structure of the substrate on the formation of the film. This influence manifests itself as the difference between the slopes of the Raman spectra, i.e., as a difference between the PL intensities. As noted above, the crystal phase of the Si substrate favors to a larger extent the formation of sp^3 -hybridized bonds. The number of π electrons and, correspondingly, the density of localized states in the band gap decrease, which contrasts with the distribution of the electron density of states in the films synthesized on quartz substrates. The decrease in the density of localized states in the band gap results in a decrease in the probability of thermalization processes and, correspondingly, in an increase in the number of radiative transitions.

Such a variation in the Raman spectra is observed in films synthesized at a specific power of the ion-plasma discharge in the range from 2.0 to 3.0 W cm^{-2} and at a Sn content up to 3.5 at % [20]. It should be noted that, if the position of the G peak corresponds to 1550 cm^{-1} or to lower frequencies, the $a\text{-C:H}\langle\text{Sn}_x\rangle$ films contain from 40 to 70% of sp^3 sites in the atomic structure; however, this statement is true for films, whose optical band gap lies in the range from 1.0 to 1.8 eV, respectively [19]. Only in this case can an amorphous diamond-like carbon matrix with a high coefficient of hardness and a high ultimate strength be formed [19].

Variations in the slope of the Raman spectrum and in the position of the G peak can be caused not only by the influence of the substrate material and the conditions of synthesis, but by the effect of the surface potential of tin nanoparticles on the formation of the atomic structure of the film as well. This inference is supported by data on the dependence of the PL intensity on the Sn content in $a\text{-C:H(Sn}_x\text{)}$ films synthesized at a specific plasma-discharge power of 2.5 W cm^{-2} (Fig. 5).

From Fig. 5, it can be seen that the PL intensity increases, as the Sn content is increased. According to the results of [21], the PL intensity of the $a\text{-C:H(Sn}_x\text{)}$ films synthesized on SiO_2 substrates at $P_d = 2.0 \text{ W cm}^{-2}$ reaches a maximum at a Sn content of $\sim 3.0 \text{ at } \%$. A further increase in the Sn content results in a decrease in the PL intensity. In [21], such behavior of the PL intensity is attributed to the change in the band gap and to the dependence of the band gap on the Sn content. The Sn content defines the nanoparticle diameter. The nanoparticle size defines the Sn modification, α - or β -Sn, which influences the formation of sp^3 - and sp^2 -type C–C bonds. In turn, the relation sp^2/sp^3 influences the formation of the density of states in the band gap. An increase or a decrease in the number of sp^2 sites yields a change in the number of π and π^* electron states that define the formation of localized states in the band gap and band-edge tails. In addition, the energy distribution of the electron density of states of Sn nanoparticles makes a substantial contribution to the formation of the energy-band edges and intraband electronic transitions.

In [21], the position of the PL intensity peak in $a\text{-C:H(Sn}_x\text{)}$ films correspond to $\sim 2.02 \text{ eV}$ and does not depend on the Sn content. As can be seen from Fig. 5, for the films synthesized on a Si(100) wafer at $P_d = 2.5 \text{ W cm}^{-2}$, the PL intensity maximum is shifted to lower energies, and its position varies under variations in the Sn content. Such an influence of Sn nanoparticles on the PL signal is defined by variations in the relation between sp^2 and sp^3 sites, sp^2/sp^3 . The PL signal corresponds to a certain configuration of sp^2 and sp^3 sites responsible for radiative electronic transitions in the band gap, with an energy in the range from 1.96 to 2.02 eV.

We attribute the decrease in the PL intensity [21] to an increase in the number of Sn nanoparticles in the β -Sn metal modification. The β -Sn modification is apparently favorable for an increase in the number of sp^2 sites, which in turn increases the density of π electron states in the band gap. The appearance of additional states in the band gap yields an increase in the probability of thermal transitions, resulting in a decrease in the PL intensity. In addition, it should be noted that metal Sn nanoparticles can be responsible

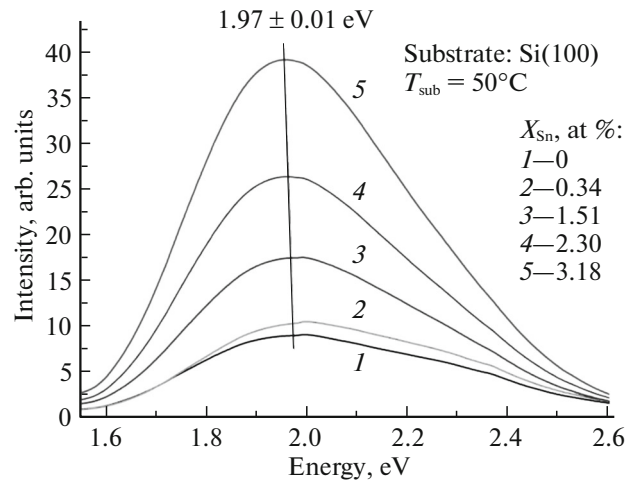


Fig. 5. PL spectra of $a\text{-C:H(Sn}_x\text{)}$ films synthesized by the DC ion-plasma method at $P_d = 2.5 \text{ W cm}^{-2}$.

for the additional localization of allowed states near the top of the valence band, specifically, for the formation of impurity centers that can cause an increase in the number of radiative transitions. An increase in the Sn content to $>3 \text{ at } \%$ [21] can yield a broadening of the energy band of states below the Fermi level, resulting in an increase in the probability of thermal transitions and, as a consequence, a decrease in the PL intensity. Thus, the PL process can involve both π electrons of sp^2 sites and electrons of β -Sn nanoparticles.

The structurally sensitive parameter that describes electronic transitions is the optical band gap E_g . Therefore, the study of the effect of Sn nanoparticles on the band gap of $a\text{-C:H}$ films can provide additional data on the formation of the electron density of states near the band edges. In amorphous semiconductors, the introduction of impurities has no effect on the band gap at low impurity concentrations and, as the impurity concentration is increased, yields a decrease in the band gap [22–26]. Tin does not form chemical bonds with carbon, and therefore, tin nanoparticles cannot directly participate in the formation of the distribution of electron states in the bands.

In this study, we determined the band gap E_g of the synthesized films from the Tauc law $\alpha hv \sim (hv - E_g)^2$ in the region of the fundamental absorption edge, at the absorption coefficient $\alpha \sim 10^5 \text{ cm}^{-1}$ and the optical density $\alpha d \sim 1$. For the $a\text{-C:H}$ film produced at $P_d = 2.5 \text{ W cm}^{-2}$, the band gap is $\sim 1.26 \text{ eV}$. The introduction of tin to a content of $\sim 1 \text{ at } \%$ increases E_g ; as the Sn content is increased further, we observe a gradual decrease in the band gap. Such a variation in E_g with X_{Sn} is observed in the films synthesized at the temperature $T_{\text{sub}} = 250^\circ\text{C}$.

Tin nanoparticles ambiguously influence the formation of the allowed band edges, which brings about several mechanisms of formation of the electron density of states. At a Sn content < 1 at %, the diameter of α -Sn nanoparticles is no larger than 10 nm, and therefore, the number of Sn atoms per particle is on average $\sim 28\,000$. At such a number of atoms, the band gap of an α -Sn nanoparticle is increased, which can cause the redistribution of electrons between the nanoparticle and the carbon matrix and a change in E_g of the a -C:H(Sn_x) film.

It is assumed that tin nanoparticles are capable of creating an additional density of allowed states above the valence-band edge and, thus, of influencing the density of π electrons that form the valence-band edge of the carbon matrix. An increase in the Sn content yields an increase in the dimensions of nanoparticles, which promotes the transition of their atomic structure to the β modification and, correspondingly, changes the energy state of electrons. In this case, the nanoparticles play the role of impurity centers. In addition, structural changes in Sn nanoparticles can substantially influence the formation of the carbon matrix and the content of sp^2 sites. This can induce a change in the distribution of the electron density of states and a decrease in the band gap.

4. CONCLUSIONS

In this study, the effect of Sn nanoparticles and of the temperature of synthesis on the structural and electronic properties of a -C:H(Sn_x) composite films is considered. A profound effect of the substrate temperature and material on the formation of the structure of the films is shown. Variations in the structure is associated with variations in the relation between the numbers of sp^2 - and sp^3 -hybridized bonds. The formation of the amorphous carbon matrix depends on the content, dimensions, and structural modification of Sn nanoparticles. Tin does not form chemical bonds with carbon atoms, but at the same time, the energy spectrum of states of Sn nanoparticles influences the electron density of states formed by π electrons of the carbon matrix. This influence is responsible for a change in the electronic properties of the a -C:H(Sn_x) film. It is shown that the PL signal greatly depends on the Sn content. It is shown that, upon the introduction of Sn to 3 at %, the PL intensity increases by a factor larger than five. Unusual optical properties are evident at Sn contents below 1.5 at %. Tin can form two different structural modifications, the α -Sn modification with semiconductor properties and the β -Sn modification with metal properties. These two modifications have different effects on the formation of the electron densities of states at the band edges and within the bands. The results of the study open up fresh opportu-

nities for modification of the properties of amorphous carbon films and for the production of composite materials with new electronic properties.

ACKNOWLEDGMENTS

The study was supported by the Science Committee, the Ministry of Education and Science of the Republic of Kazakhstan, project no. 3219/GF.

REFERENCES

1. A. Erdemir and Ch. Donnet, *J. Phys. D: Appl. Phys.* **39**, R311 (2006).
2. M. Suzuki, T. Ohana, and A. Tanaka, *Diamond Relat. Mater.* **13**, 2216 (2004).
3. R. A. Andrievskiy, *Russ. Chem. Rev.* **66**, 53 (1997).
4. A. P. Ryaguzov, G. A. Yermekov, R. R. Nemkayeva, N. R. Guseinov, and R. K. Aliaskarov, *J. Mater. Res.* **31**, 127 (2016).
5. A. D. Korotaev, S. V. Ovchinnikov, A. N. Tyumentsev, Yu. P. Pinzhin, G. Yu. Yushkov, A. G. Nikolaev, and K. P. Savkin, *Poverkhnost'*, No. 1, 46 (2004).
6. Š. Meškiniš, A. Čiegis, A. Vasiliauskas, K. Šlapikas, T. Tamulevičius, A. Tamulevičienė, and S. Tamulevičius, *Thin Solid Films* **581**, 48 (2014).
7. Ye. J. Jo, T. F. Zhang, M. J. Son, and K. H. Kim, *Appl. Surf. Sci.* **433**, 1184 (2018).
8. B. F. Dorfman, *Thin Solid Films* **330**, 76 (1998).
9. Sh. Sh. Sarsembinov, O. Yu. Prikhodko, A. P. Ryaguzov, S. Ya. Maksimova, Ye. A. Daineko, and F. A. Mahmoud, *Phys. Status Solidi C* **7**, 805 (2010).
10. T. Acsente, E. R. Ionita, D. Colceag, A. Moldovan, C. Luculescu, R. Birjega, and G. Dinescu, *Thin Solid Films* **519**, 4054 (2011).
11. A. Chandrashekar, S. Ramachandran, G. Pollack, J. S. Lee, G. S. Lee, and L. Overzet, *Thin Solid Films* **517**, 525 (2008).
12. X. M. Dong, Y. Luo, L. N. Xie, R. W. Fu, and M. Q. Zhang, *Thin Solid Films* **516**, 7886 (2008).
13. G. Yar-Mukhamedova, G. Ismailova, A. Markhabaeva, and A. Darisheva, *Asian J. Nat. Appl. Sci.* **3**, 61 (2014).
14. F. F. Komarov, G. A. Ismailova, O. V. Mil'chanin, I. N. Parkhomenko, F. B. Zhushipbekova, and G. Sh. Yar-Mukhamedova, *Tech. Phys.* **60**, 1348 (2015).
15. A. C. Ferrari and J. Robertson, *Phys. Rev. B* **61**, 14095 (2000).
16. D. S. Knight and W. B. White, *J. Mater. Res.* **4**, 385 (1989).
17. A. P. Ryaguzov, B. E. Alpysbayeva, R. R. Nemkayeva, R. K. Aliaskarov, D. M. Mamyrbayeva, and O. I. Yukhnovets, *Eur. Phys. Tech. J.* **13**, 52 (2016).
18. F. Tuinstra and J. L. Koenig, *J. Chem. Phys.* **53**, 1126 (1970).

19. A. C. Ferrari and J. Robertson, *Philos. Trans. R. Soc.* **362**, 2477 (2004).
20. A. P. Ryaguzov, R. R. Nemkaeva, N. R. Guseinov, and D. M. Mamyrbayeva, in *Proceedings of the 2nd International Conference on Modern Technologies in Science and Education, Ryazan, March 1–3, 2017*, Ed. by O. V. Milovzorov (Ryazan. Gos. Radiotekh. Univ., Ryazan', 2017), p. 191.
21. A. P. Ryaguzov, R. R. Nemkaeva, N. R. Guseinov, and D. M. Mamyrbayeva, in *Proceedings of the 2nd International Conference on Modern Technologies in Science and Education, Ryazan, March 1–3, 2017*, Ed. by O. V. Milovzorov (Ryazan. Gos. Radiotekh. Univ., Ryazan', 2017), p. 182.
22. A. Marchenko, N. Anisimova, A. Naletko, T. Rabchanova, P. Seregin, and H. Ali, *Glass Phys. Chem.* **39**, 287 (2013).
23. S. Coffa, S. Lombardo, F. Priolo, G. Franzó, S. U. Campisano, A. Polman, and G. N. van den Hoven, *Nuovo Cim. D* **18**, 1131 (1996).
24. P. Brogueira, V. Chu, A. C. Ferro, and J. P. Conde, *J. Vac. Sci. Technol., A* **15**, 2968 (1997).
25. S. Meskinis, R. Gudaitis, A. Vasiliasauskas, A. Ciegis, K. Slapikas, T. Tamulevicius, M. Andrulevicius, and S. Tamulevicius, *Diamond Relat. Mater.* **60**, 20 (2005).
26. D. I. Jones and A. D. Stewart, *Phil. Mag. B* **46**, 423 (1982).

Translated by E. Smorgonskaya